nanomaterials

MDPI

Article

H_2 Plasma and PMA Effects on PEALD-Al_2O_3 Films with Different O_2 Plasma Exposure Times for CIS Passivation Layers

Jehyun An [1], Kyeongkeun Choi [2], Jongseo Park [1], Bohyeon Kang [1], Hyunseo You [1], Sungmin Ahn [1] and Rockhyun Baek [1,*]

[1] Department of Electrical Engineering, Pohang University of Science and Technology (POSTECH), Pohang 37673, Republic of Korea
[2] National Institute for Nanomaterials Technology (NINT), Pohang University of Science and Technology (POSTECH), Pohang 37673, Republic of Korea
* Correspondence: rh.baek@postech.ac.kr; Tel.: +82-54-279-2220

Abstract: In this study, the electrical properties of Al_2O_3 film were analyzed and optimized to improve the properties of the passivation layer of CMOS image sensors (CISs). During Al_2O_3 deposition processing, the O_2 plasma exposure time was adjusted, and H_2 plasma treatment as well as post-metallization annealing (PMA) were performed as posttreatments. The flat-band voltage (V_{fb}) was significantly shifted (ΔV_{fb} = 2.54 V) in the case of the Al_2O_3 film with a shorter O_2 plasma exposure time; however, with a longer O_2 plasma exposure time, V_{fb} was slightly shifted (ΔV_{fb} = 0.61 V) owing to the reduction in the carbon impurity content. Additionally, the as-deposited Al_2O_3 sample with a shorter O_2 plasma exposure time had a larger number of interface traps (interface trap density, $D_{it} = 8.98 \times 10^{13}$ $eV^{-1} \cdot cm^{-2}$). However, D_{it} was reduced to 1.12×10^{12} $eV^{-1} \cdot cm^{-2}$ by increasing the O_2 plasma exposure time and further reduced after PMA. Consequently, we fabricated an Al_2O_3 film suitable for application as a CIS passivation layer with a reduced number of interface traps. However, the Al_2O_3 film with increased O_2 plasma exposure time deteriorated owing to plasma damage after H_2 plasma treatment, which is a method of reducing carbon impurity content. This deterioration was validated using the C–V hump and breakdown characteristics.

Keywords: high-k gate dielectric; Al_2O_3; H_2 plasma treatment; interface trap; plasma-enhanced atomic layer deposition

Citation: An, J.; Choi, K.; Park, J.; Kang, B.; You, H.; Ahn, S.; Baek, R. H_2 Plasma and PMA Effects on PEALD-Al_2O_3 Films with Different O_2 Plasma Exposure Times for CIS Passivation Layers. *Nanomaterials* **2023**, *13*, 731. https://doi.org/10.3390/nano13040731

Academic Editor: Andrei Ionut Mardare

Received: 30 January 2023
Revised: 11 February 2023
Accepted: 13 February 2023
Published: 14 February 2023

1. Introduction

Recently, the importance of CMOS image sensor (CIS) technology has rapidly increased owing to its relevance in mobile products and autonomous driving. As electronic products become ever-smaller in size, smaller CIS devices are also required. Therefore, CIS devices must be scaled, similar to other semiconductor devices. The pixel size of the CIS image sensor has been rapidly scaled, limiting the number of photons entering the pixel. In addition, as a result of scaling, light reflection occurred, causing light loss and cross-talk issues [1]. Therefore, a backside illumination-type CIS device that illuminates the rear side of the device was developed [2]. However, the backside illumination structure is adversely affected by dark currents and noise. Hence, in order to decrease dark current and increase quantum efficiency, research on the development of high-k materials for application as a CIS passivation dielectric layer is necessary.

Al_2O_3, which is a high-k dielectric material, has a wide energy bandgap and high thermal stability; therefore, it is suitable for application as a passivation dielectric film for CIS [3,4]. In addition, unlike other dielectric films, Al_2O_3 has negative fixed charges and shows excellent passivation characteristics [5]. In most semiconductor devices such as complementary metal oxide semiconductors (CMOSs), fixed charges act as defects [6]. Thus, many studies have been conducted to control these negative fixed charges [7]. However, in

the CIS device, a passivation dielectric layer is required to contain high fixed charges for field effect passivation. Therefore, Al_2O_3 is a suitable dielectric material as a passivation layer of CIS. However, a dielectric film with fewer impurities is required for fabricating a more precise CIS device, and defects in Al_2O_3 must be further cured. In particular, for application as a dielectric film, the interface trap density (D_{it}) should be reduced to increase the amount of light absorbed. There are several causes of trap generation in the interface area between Al_2O_3 dielectric and substrate. If the Al_2O_3 dielectric is deposited on the silicon substrate, the hydroxyl group (-OH) and Si are bonded, which may act as an interface trap [8]. In another case, carbon impurities generated during the Al_2O_3 deposition process act as interface traps.

Carbon impurities were generated after the Al_2O_3 film was deposited via plasma-enhanced atomic layer deposition (PEALD) using trimethylaluminum as a precursor [9]. These impurities act as traps inside the Al_2O_3 and in the interface region. Previously, residual carbon was removed using the H_2 plasma treatment of an Al_2O_3 film [10]. The quality of the dielectric and interface areas increased with a decrease in carbon impurity contents. In addition, posttreatments provided sufficient fixed charges for the Al_2O_3 dielectric to be used as the passivation layer of the CIS [11,12]. However, a low D_{it} is required for next-generation CIS devices. Although well-known defects, such as oxygen vacancies, have been investigated [13], limited studies have been conducted to reduce residual carbon contents, except by changing the precursor [14].

In this study, the oxygen plasma exposure time was adjusted during Al_2O_3 deposition to reduce the residual carbon content. The increased O_2 plasma exposure time sufficiently decreased the D_{it} of the Al_2O_3 gate stack. Consequently, it showed a considerably lower D_{it} compared with that of the sample processed via rapid thermal annealing and H_2 plasma treatment on Al_2O_3, which exhibited the lowest D_{it} in a previous study [10]. In particular, D_{it} was the lowest after post-metallization annealing (PMA) to Al_2O_3 samples with increased O_2 plasma exposure time. In addition, a positive shift in flat-band voltage (ΔV_{fb}) was prevented by reducing carbon generation. However, D_{it} increases when H_2 plasma treatment is performed after Al_2O_3 deposition. Plasma damage and residual hydrogen impurities were caused by excessive H_2 plasma treatment on Al_2O_3 dielectric and were validated using the C–V hump occurring in the capacitance vs. voltage (C–V_G) measurement curve.

2. Experimental Materials and Methods

As shown in Figure 1, an Al_2O_3 film was deposited on a Si substrate at 275 °C using PEALD. Substrate included moderately doped p-type Si (1–30 Ω·cm, (100)) with a doping concentration of ~1.3×10^{16} cm^{-3}. Prior to deposition of the Al_2O_3 layer, Si substrates were cleaned by dipping in a NH_4OH:H_2O_2:H_2O mixture (1:1:5 by volume), known as Standard Clean 1 (SC1), for 10 min at 70 °C, followed by dipping in dilute HF (100:1) for 1 min to remove native oxides. For deposition of Al_2O_3 dielectric, a commercial 200 mm wafer plasma-enhanced vapor deposition (PECVD; Quros Plus 200) was used. As a precursor, Trimethylaluminum (TMA, $Al(CH_3)_3$) (Up chemical co. Ltd., Pyeongtaek, Gyeonggi-do, Republic of Korea; 99.9999%) was supplied. For sequential surface reactions, O_2 plasma was supplied with TMA. The O_2 plasma exposure times were 3 and 7 s. During the deposition, an $Al(CH_3)_3$ container temperature of 25 °C, an Ar purge flow rate of 500 sccm, an O_2 flow rate of 100 sccm and a chamber pressure of 0.4 mTorr were used. Al electrode with a diameter of 300 μm and an area of 7.06×10^4 μm^2 was deposited on the Al_2O_3 dielectric using an e-beam evaporator. The thickness of the Al_2O_3 film was measured using transmission electron microscopy (TEM; JEM-2100F; JEOL KOREA LTD., Seoul, Republic of Korea) and ellipsometry (M-2000; J. A. Woollam Co., Anyang, Gyeonggi-do, Republic of Korea). After Al_2O_3 deposition, H_2 plasma treatment and PMA were performed separately depending on the sample (Table 1). H_2 plasma treatment was performed with a H_2 gas flow rate ratio {[H_2] = ([H_2] + [Ar])} of 0.89 in a PECVD chamber for 15 min. PMA was performed at 400 °C under a N_2 gas flow in a furnace for 30 min. The N_2 gas flow

rate {[N_2] = ([N_2] + [H_2])} was 0.95 (gas pump: 100 sccm; pressure: 0.7 atm). Under the N_2 gas flow, the temperature increased from 25 °C to 400 °C in 1 h and then decreased from 400 °C to 25 °C in 2 h. Secondary ion mass spectrometry (SIMS) measurements were conducted on a circular area with a diameter of 33 µm using the Cs+ software. Selective area diffraction pattern (SADP) analysis was carried out to determine crystallinity of the Al_2O_3 film. The capacitance and conductance were measured using a B1520A multifrequency capacitance measurement unit at various frequencies (1 kHz–1 MHz). The leakage current and breakdown field were measured using a Keithley 4200-SCS instrument (Tektronix KOREA, Seoul, Republic of Korea). D_{it} ($\approx 2.5(qA)^{-1}(G_p/\omega)_{max}$) was calculated following the well-known conductance method [15]:

$$G_p/\omega = C_{OX}^2 G_M \omega^{-1} / \left\{ (G_M/\omega)^2 + (C_{OX} - C_M)^2 \right\} \quad (1)$$

where q = 1.6×10^{19} C; A is the area of the electrode; $(G_p/\omega)_{max}$ is the normalized parallel conductance peak; C_{OX} is the capacitance in strong accumulation; C_M is the measured capacitance; and G_M is the measured conductance.

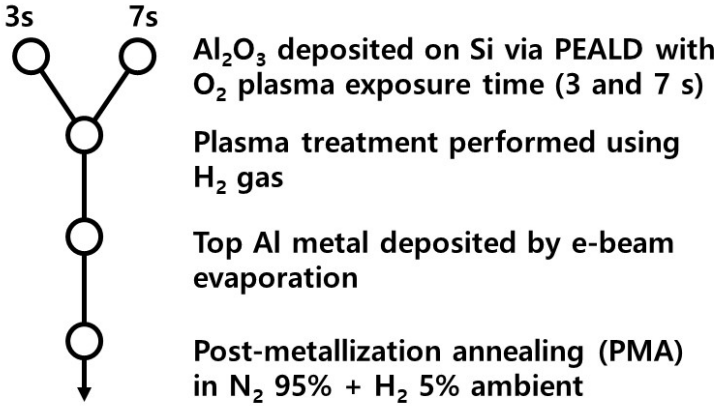

Figure 1. Process flow for the fabrication of the Al/Al_2O_3/Si gate stack.

Table 1. Al_2O_3 samples under deposition conditions (O_2 plasma exposure time: 3 and 7 s) and posttreatment conditions (H_2 plasma treatment and post-metallization annealing (PMA)).

Samples	O_2 Plasma Exposure Time (s)	H_2 Plasma Treatment	PMA
S1_as_dep	3	X	X
S1_H_2_plamsa	3	O	X
S1_PMA	3	X	400 °C; 30 min
S1_H_2 plasma + PMA	3	O	400 °C; 30 min
S2_as_dep	7	X	X
S2_H_2_plamsa	7	O	X
S2_PMA	7	X	400 °C; 30 min
S2_H_2 plasma + PMA	7	O	400 °C; 30 min

3. Results and Discussion

3.1. Post-Metallization Annealing

Al_2O_3 was deposited via PEALD using trimethylaluminum as the precursor and O_2 plasma. A flux of O* radicals reacts with methyl groups and is effused in the CO_X (x = 1–2) state [16]. However, residual carbon is generated when a sufficient reaction is not performed and acts as a defect in the inner and interfacial regions of Al_2O_3. Accordingly, the O_2 plasma exposure time was increased to 7 s to ensure a sufficient response.

The TEM image of the as-deposited Al_2O_3 film is shown in Figure 2a. An Al_2O_3 film with a thickness of 30 nm was deposited on the Si substrate, and Al electrode was deposited

on the Al_2O_3 dielectric. No interfacial layer (IL) was formed at the interface between Si and Al_2O_3. Additionally, based on the SADP in Figure 2a, the as-deposited Al_2O_3 is in an amorphous state.

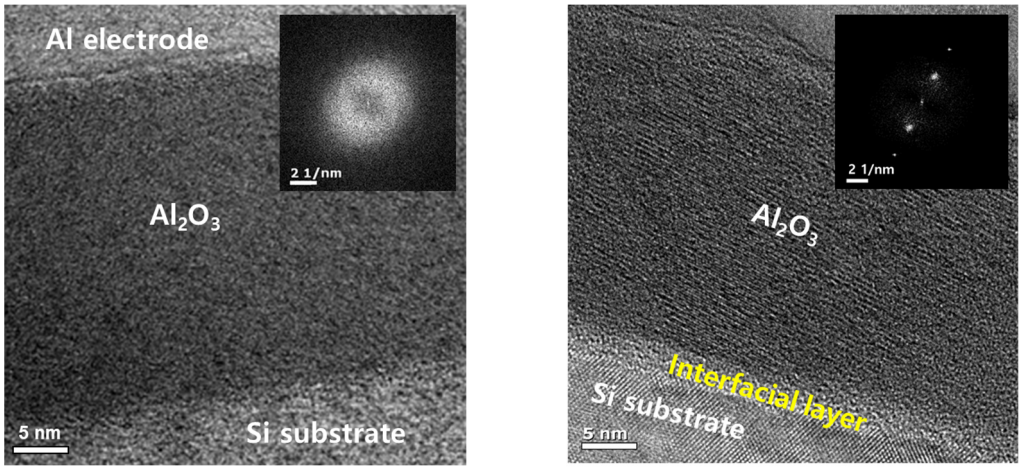

(**a**) (**b**)

Figure 2. Transmission electron microscope (TEM) image and selective area diffraction pattern (SADP) of (**a**) as-deposited Al/Al_2O_3/Si gate stack and (**b**) Al/Al_2O_3/Si gate stack after PMA at 400 °C under a N_2 gas flow in a furnace for 30 min.

PMA was performed at 400 °C for 30 min after Al_2O_3 film deposition. After PMA on the Al_2O_3 film, oxygen in the dielectric film diffused toward the Si substrate. Accordingly, Si and oxygen form a bond in the SiO_X (x = 1–2) state, thereby forming an IL with a thickness of 2.5 nm [8,17] (Figure 2b). As IL was formed between Al_2O_3 and Si, the thickness of Al_2O_3 decreased from 28.7 to 26.9 nm after PMA. Furthermore, as shown in SADP, amorphous Al_2O_3 is converted to polycrystalline Al_2O_3 via PMA [18].

The normalized capacitance vs. voltage curves before and after PMA of S1 and S2 are shown in Figure 3. The graphical $((C_{OX}/C_{MOS})^2 - 1)(V_G)$ method [19] was applied to the normalized capacitance vs. voltage curve to extract V_{fb}. The V_{fb} of as-deposited S1 was 1.65 V, showing a considerable flat-band voltage shift ($\Delta V_{fb} \approx 2.54$ V) compared with the theoretical value of Al_2O_3 dielectric ($V_{fb} \approx -0.89$ V). This V_{fb} shift resulted from defects, such as carbon impurities that occur during Al_2O_3 deposition via PEALD. However, in the case of S2 samples with an increased O_2 plasma exposure time, the V_{fb} of S2_as_dep is 0.61 V, exhibiting a smaller ΔV_{fb} compared with that of S1. This is because the amount of negatively charged defects inside S2 is smaller than that of S1.

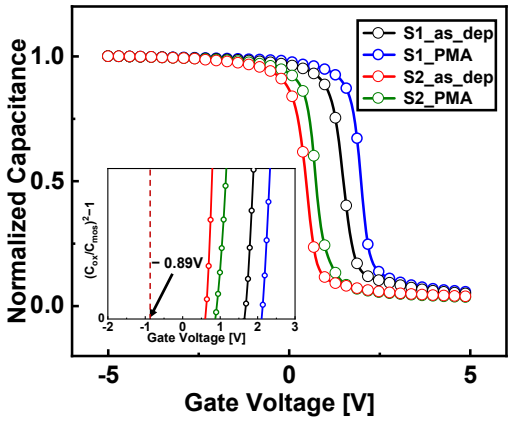

Figure 3. Normalized capacitance vs. voltage graph and graphical $((C_{OX}/C_{MOS})^2 - 1)(V_G)$ method to extract the flat-band voltage (V_{fb}) of Al_2O_3 samples with and without PMA (frequency = 1 MHz).

V_{fb} increased by 0.54 V after PMA in the case of Al_2O_3 samples with short O_2 plasma exposure times. Internal defects that form bonds with carbon impurities have a negative charge and diffuse toward Si [10,14]. However, in the case of S2 samples with long O_2 plasma exposure times, the change in V_{fb} was as small as 0.2 V owing to a decrease in the defects that can be diffused.

The permittivity of Al_2O_3 samples before and after PMA is shown in Figure 4. The permittivity is 9.5 in the case of the as-deposited S1 sample, which is similar to the generally known permittivity value of amorphous Al_2O_3 (6–9) [18,20]. However, an IL of SiO_X (x = 1–2) is formed between Al_2O_3 and Si after PMA, slightly decreasing the permittivity. The permittivity of the as-deposited S2 sample is 12.5, which is considerably higher than that of the S1 sample. This is because of the decrease in the content of various defects and the increase in the internal carbon concentration owing to the longer O_2 plasma exposure time. After PMA on the as-deposited S2 sample, the permittivity decreases to 10.5 because an IL of SiOx (x = 1–2) is formed between Al_2O_3 and Si like the S1 sample. However, the S2_PMA sample still showed a higher permittivity than the S1 samples with shorter O_2 plasma exposure time.

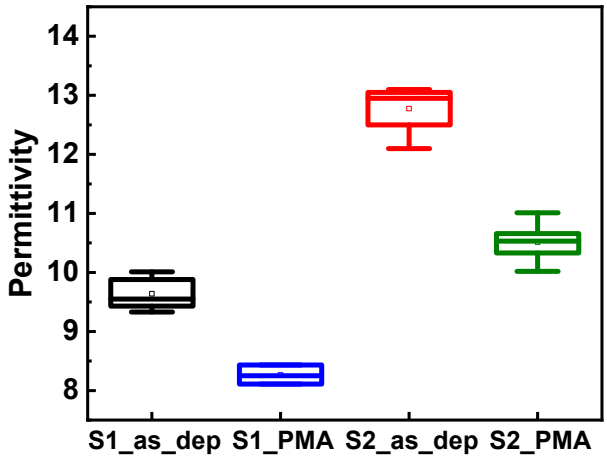

Figure 4. Permittivity of Al_2O_3 samples under deposition conditions (O_2 plasma exposure time: 3 and 7 s) and post-metallization annealing (PMA).

The decrease in the carbon impurity content with increasing O_2 plasma exposure time was validated using SIMS depth profiling. As shown in Figure 5, the amount of carbon impurities in the Al_2O_3 film deposited with an O_2 plasma exposure time of 7 s is considerably less than that of the Al_2O_3 sample deposited with a shorter O_2 plasma exposure time. As the O_2 plasma exposure time increased, more carbon was effused into the CO_X (x = 1–2) gas state through numerous reactions between the oxygen plasma and carbon [16]. If the O_2 plasma exposure time is more than 7 s, there is a possibility of improvement as much as carbon is reduced. However, there is a limit to effuse through the reaction with carbon, and the improvement effect is expected to be saturated as carbon is reduced.

To apply Al_2O_3 as a passivation dielectric film, the quality of the interface region between Si and Al_2O_3 is crucial. Carbon in Al_2O_3 acts as an interface trap in the interface region between the Al_2O_3 dielectric and Si substrate [21]. The parallel conductance versus frequency plots of the Al_2O_3 films with various D_{it} values are shown in Figure 6. D_{it} was measured using the conductance method [13]. The D_{it} of the S1_as_dep sample was 8.98×10^{13} $eV^{-1} \cdot cm^{-2}$, whereas that of the S2_as_dep sample was 1.12×10^{12} $eV^{-1} \cdot cm^{-2}$. The interface traps of the S2 sample decreased with a decrease in the carbon impurity content in the interface area with increasing O_2 plasma exposure time. After PMA, the interface region between the Al_2O_3 dielectric and Si was improved due to various reasons. First, an IL was formed after the application of PMA to the Al_2O_3 gate stack. Therefore, the number of hydroxyl groups is reduced, thereby decreasing the number of interface traps [22]. For

other reason, as crystallization of Al_2O_3 occurred due to PMA, defects and dangling bonds acting as traps in the interface region were removed. In addition, crystallization of the Al_2O_3 dielectric stabilized the bond between the Al_2O_3 and Si substrate [10].

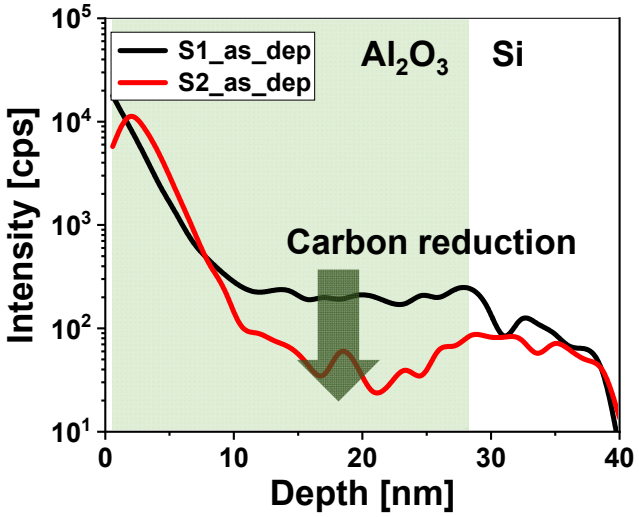

Figure 5. Secondary ion mass spectrometry (SIMS) depth profiles of carbon in the Al/Al_2O_3/Si gate stack with an O_2 plasma exposure time of 3 (black line) and 7 s (red line).

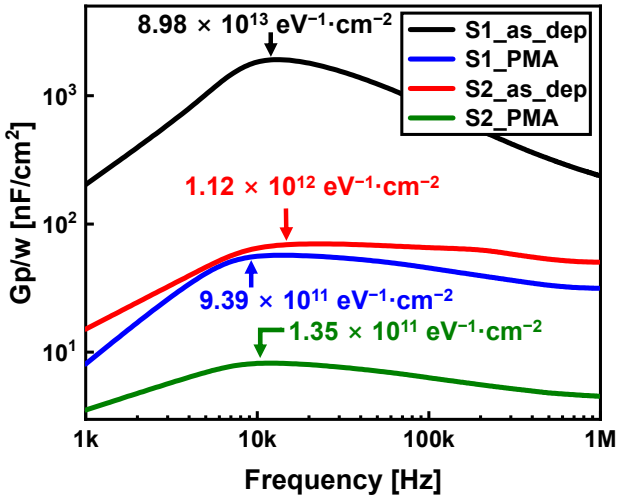

Figure 6. G_P/w vs. frequency curves of Al_2O_3 samples with and without PMA for measuring interface trap density (D_{it}).

In summary, the number of interface traps of the S2_PMA sample, in which the concentrations of both carbon impurities and hydroxyl groups were reduced, were the lowest in this study ($D_{it} = 1.35 \times 10^{11}$ $eV^{-1} \cdot cm^{-2}$).

The interface improvement owing to the increase in the O_2 plasma exposure time was also validated using the breakdown characteristics. The gate leakage current with an increase in the electrical field of the S1 and S2 Al_2O_3 samples is shown in Figure 7a. In the case of S1_as_dep, the breakdown occurred at 9.73 MV/cm. The breakdown characteristics improved after PMA was performed owing to the formation of an IL, which occurred at 11.47 MV/cm. However, breakdown did not occur until the application of the maximum electric field (14 MV/cm) of the 4200-SCS equipment in the case of the S2 sample. Furthermore, breakdown did not occur in the case of the S2_as_dep sample without the IL. This was because of the reduction in the impurity content in the interface area with an increase in the O_2 plasma exposure time.

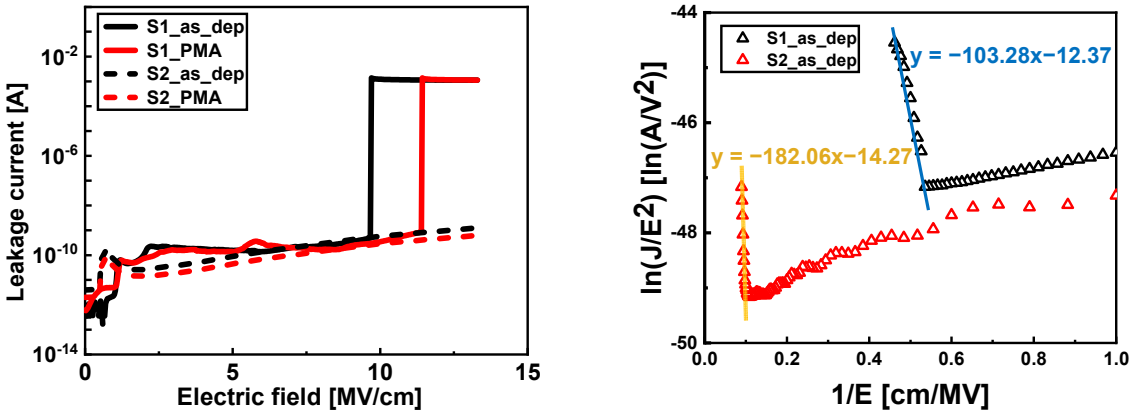

(**a**) (**b**)

Figure 7. (**a**) Leakage current vs. gate electric field of Al_2O_3 samples with and without PMA. (**b**) Fowler–Nordheim (FN) plots of I–V curves for as-deposited Al_2O_3 samples with an O_2 plasma exposure time of 3 (black triangles) and 7 s (red triangles).

In addition, the FN plots to validate the improvement in the interface quality are shown in Figure 7b. The FN plot is analyzed using the leakage current density caused by FN tunneling, J_{FN}, and can be described as follows:

$$J_{FN} = AE^2 \exp(-B/E), \quad (2)$$

where

$$A = q^3 m_0/(8\pi h m^* \Phi_B),$$

and

$$B = 4(2m^*)^{\frac{1}{2}}(q\Phi_B)^{\frac{3}{2}}/(3qh/2\pi),$$

where A is the Richardson's constant; q is the electronic charge; h is Planck's constant; m_0 is the free electron mass; m^* is the effective electron mass in the oxide; and Φ_B is the barrier height [23]. The steeper the slope in the FN plot, the larger the FN barrier height Φ_B [4]. Since the absolute value of the slope of the S2_as_dep sample (slope = −182.06) is larger than that of the S1_as_dep sample (slope = −103.28), it means that the barrier height is higher in S2_as_dep. Therefore, the FN plot shows that the interface region of Al_2O_3/Si was improved in the S2 sample with increased O_2 plasma exposure time.

In summary, the increase in the O_2 plasma exposure time decreases the carbon content in Al_2O_3, which reduces D_{it}, improves the breakdown field, and prevents the V_{fb} shift. However, the H_2 plasma treatment decreased the quality of the oxide and interface owing to the increase in the O_2 plasma exposure time, which is discussed later.

3.2. H_2 Plasma Treatment

H_2 plasma treatment significantly decreased the carbon impurity content in Al_2O_3 in previous studies [10], thereby preventing the V_{fb} shift and improving the breakdown characteristics. However, further improvements in the interface quality is required for next-generation CIS devices. Therefore, we analyzed the effects of the H_2 plasma treatment on Al_2O_3 films with increasing O_2 plasma exposure time.

D_{it} values depending on various treatments on the Al_2O_3 samples are shown in Figure 8. The average D_{it} of the sample with the H_2 plasma treatment was 4.45×10^{12} $eV^{-1} \cdot cm^{-2}$, which was significantly smaller than that of as-deposited S1. However, the average D_{it} of the sample with the H_2 plasma treatment was 1.13×10^{12} $eV^{-1} \cdot cm^{-2}$ in the case of S2 samples with an increased O_2 plasma exposure time, which increased compared with the average D_{it} of as-deposited S2 ($D_{it,as\_dep\ S2} = 5.79 \times 10^{11}$ $eV^{-1} \cdot cm^{-2}$). A

similar trend was observed after PMA. D_{it} was higher in the S2 sample with the H_2 plasma treatment and PMA than that of the S2 sample treated with only PMA.

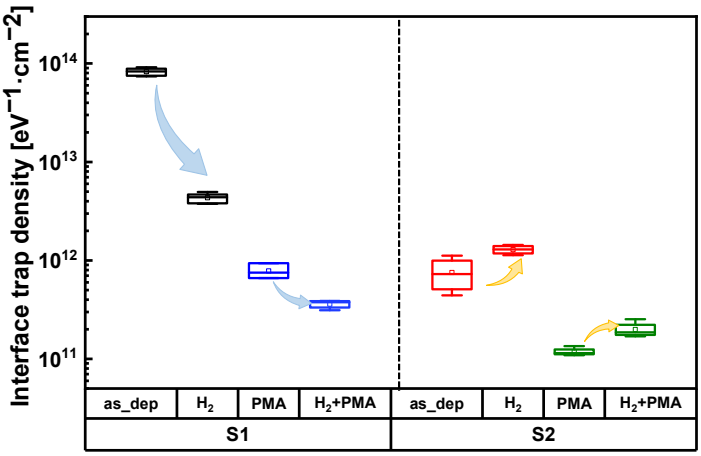

Figure 8. Interface trap density (D_{it}) of Al_2O_3 samples under deposition conditions; O_2 plasma exposure time: 3 (**left** side) and 7 s (**right** side) and posttreatment conditions: H_2 plasma treatment and post-metallization annealing (PMA).

A large amount of carbon impurities was removed owing to the increased O_2 plasma exposure time in the S2 sample. Therefore, there are not enough carbon impurities for the reaction with the H_2 plasma. As a result, owing to the excessive postprocessing H_2 plasma treatment on the S2 sample, H impurities remained inside the Al_2O_3 film [24]. In addition, additional H_2 plasma treatment for carbon impurities, whose content was reduced owing to an increase in the O_2 plasma exposure time, had a more significant effect on the formation of defects owing to damage due to the plasma treatment compared with the effects of curing defects owing to carbon content reduction [25]. In conclusion, in the case of the S2 sample with increased O_2 plasma exposure time, excessive postprocessing H_2 plasma treatment caused residual H impurities and plasma damage, which contributed to increase D_{it} by forming dangling bonds in interface region.

Using the capacitance vs. voltage curve, the plasma damage to the gate stack was confirmed. The normalized capacitance before and after the H_2 plasma treatment in the S2 sample with an increased O_2 plasma exposure time is shown in Figure 9. In contrast to the S2_as_dep sample, the C–V hump occurs near V_{fb} in the S2_H_2 plasma sample. Therefore, the hydrogen plasma, which should be effused via the reaction with carbon, damaged the Al_2O_3 dielectric.

The formation of defects in the oxide and interface regions of the S2 sample owing to the H_2 plasma treatment resulted in more leakage flow in the gate stack. In contrast to the S2_as_dep sample, where breakdown does not occur even under the electric field limit of the 4200-SCS equipment (E_{field} = 14 MV/cm), the breakdown occurs at 11.2 MV/cm in the S2_H_2 plasma sample (Figure 10). As a result, in the case of the Al_2O_3 film with increased O_2 plasma exposure time, H_2 plasma treatment rather deteriorates the interface quality between Al_2O_3 dielectric and Si.

In summary, H_2 plasma treatment has different effects depending on the O_2 plasma exposure time during deposition of the Al_2O_3 dielectric. H_2 plasma treatment was effective for S1 samples with a large amount of carbon impurities because of the short O_2 plasma exposure time. Due to the reduction of carbon impurities, the D_{it} of the S1 sample was greatly reduced after H_2 plasma treatment. However, the treatment effects on S2 samples was rather poor, resulting in reduced carbon content owing to the long O_2 plasma exposure time. H_2 plasma treatment produced residual H impurities in the S2 samples and also caused plasma damage. Therefore, H_2 plasma treatment rather increased D_{it} in the Al_2O_3 with increased O_2 plasma exposure time.

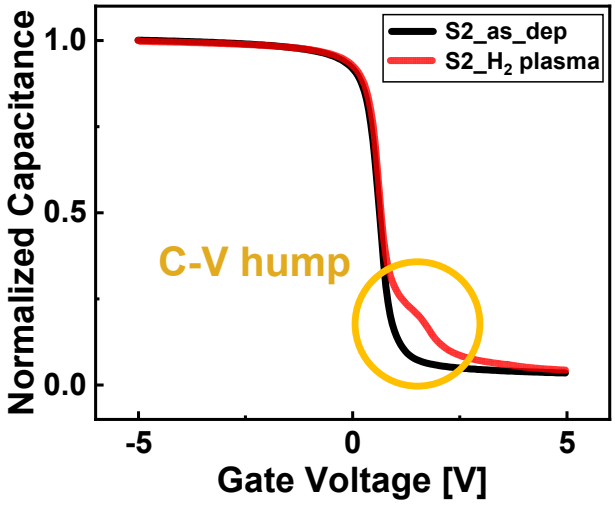

Figure 9. C–V hump effect (yellow circle) owing to excessive H_2 plasma treatment in the normalized capacitance vs. voltage curves of Al_2O_3 films with an increased O_2 plasma exposure time (frequency = 1 MHz).

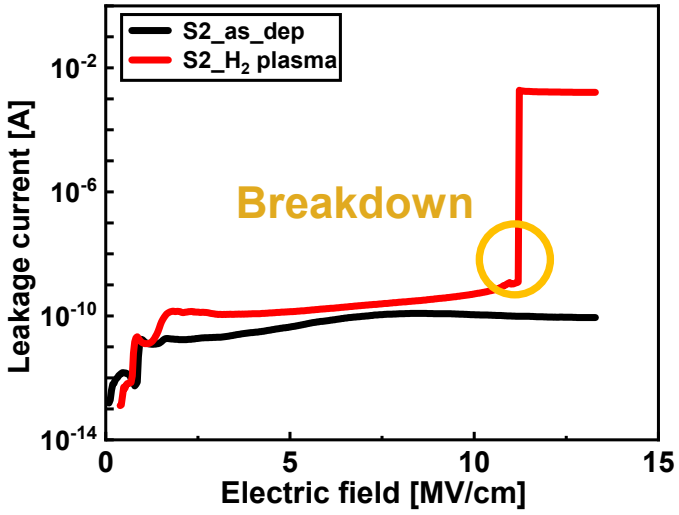

Figure 10. Leakage current vs. gate electric field of Al_2O_3 samples with an increased O_2 plasma exposure time.

4. Conclusions

The criterion of fixed charges in the Al_2O_3 film for application as a CIS passivation layer was satisfied in a previous study; however, the issue of interface traps remained unresolved. Further improvement in the interface area is required for Al_2O_3 to be used as a passivation dielectric layer. Therefore, this study investigated the conditions to reduce defect contents and the D_{it} of the Al_2O_3 film. The carbon content inside the Al_2O_3 was significantly decreased by adjusting the O_2 plasma exposure time to induce more reactions during dielectric deposition. D_{it} was significantly decreased owing to the reduction in the amount of carbon impurities, and the improvement in the interface region was validated using the breakdown characteristics. Moreover, H_2 plasma treatment effectively reduced D_{it} in Al_2O_3 films with a short O_2 plasma exposure time during deposition. However, H_2 plasma treatment of the Al_2O_3 film deposited with a long O_2 plasma exposure time rather increased D_{it} due to plasma damage. PMA slightly decreased the permittivity after Al_2O_3 deposition; however, D_{it} significantly decreased. In particular, in the case of Al_2O_3 samples with increased O_2 plasma exposure time, after PMA, it had the lowest D_{it}, which is suitable for use as a passivation layer for CIS.

Author Contributions: Conceptualization, J.A.; methodology, J.A., K.C., J.P. and B.K.; formal analysis, J.A.; investigation, J.A., J.P., B.K. and H.Y.; resources, K.C.; data curation, J.A. and J.P.; writing—original draft preparation, J.A.; writing—review and editing, J.P., B.K., H.Y. and S.A.; supervision, S.A. and R.B.; project administration, R.B.; funding acquisition, R.B. All authors have read and agreed to the published version of the manuscript.

Funding: This study was supported by the Ministry of Trade, Industry, and Energy (MOTIE) (20010574, 20019450, 20020286); the Korea Semiconductor Research Consortium (KSRC) support program for the development of future semiconductor devices; and a National Research Foundation of Korea (NRF) grant funded by the Korean government (MSIT) (No. NRF-2020R1A4A4079777 and NRF-2020M3F3A2A02082436) and BK21 FOUR program.

Data Availability Statement: Not applicable.

Acknowledgments: Not applicable.

Conflicts of Interest: The authors declare no conflict of interest.

References

1. Agranov, G.; Berezin, V.; Tsai, R.H. Crosstalk and Microlens Study in a Color CMOS Image Sensor. *IEEE Trans. Electron Devices* **2003**, *50*, 4–11. [CrossRef]
2. Wuu, S.G.; Wang, C.C.; Hseih, B.C.; Tu, Y.L.; Tseng, C.H.; Hsu, T.H.; Hsiao, R.S.; Takahashi, S.; Lin, R.J.; Tsai, C.S.; et al. A Leading-Edge 0.9 μm Pixel CMOS Image Sensor Technology with Backside Illumination: Future Challenges for Pixel Scaling. *Tech. Dig.-Int. Electron Devices Meet. IEDM* **2010**, *332–335*, 14.1.1–14.1.4. [CrossRef]
3. Wilk, G.D.; Wallace, R.M.; Anthony, J.M. High-κ Gate Dielectrics: Current Status and Materials Properties Considerations. *J. Appl. Phys.* **2001**, *89*, 5243–5275. [CrossRef]
4. Groner, M.D.; Elam, J.W.; Fabreguette, F.H.; George, S.M. Electrical Characterization of Thin Al_2O_3 Films Grown by Atomic Layer Deposition on Silicon and Various Metal Substrates. *Thin Solid Films* **2002**, *413*, 186–197. [CrossRef]
5. Dingemans, G.; Kessels, W.M.M. Status and Prospects of Al_2O_3 -Based Surface Passivation Schemes for Silicon Solar Cells. *J. Vac. Sci. Technol. A Vac. Surf. Film.* **2012**, *30*, 040802. [CrossRef]
6. Kühnhold-Pospischil, S.; Saint-Cast, P.; Richter, A.; Hofmann, M. Activation Energy of Negative Fixed Charges in Thermal ALD Al_2O_3. *Appl. Phys. Lett.* **2016**, *109*, 061602. [CrossRef]
7. Buckley, J.; De Salvo, B.; Deleruyelle, D.; Gely, M.; Nicotra, G.; Lombardo, S.; Damlencourt, J.F.; Hollinger, P.; Martin, F.; Deleonibus, S. Reduction of Fixed Charges in Atomic Layer Deposited Al_2O_3 Dielectrics. *Microelectron. Eng.* **2005**, *80*, 210–213. [CrossRef]
8. Uenuma, M.; Takahashi, K.; Sonehara, S.; Tominaga, Y.; Fujimoto, Y.; Ishikawa, Y.; Uraoka, Y. Influence of Carbon Impurities and Oxygen Vacancies in Al_2O_3 Film on Al_2O_3/GaN MOS Capacitor Characteristics. *AIP Adv.* **2018**, *8*, 105103. [CrossRef]
9. Puurunen, R.L. Surface Chemistry of Atomic Layer Deposition: A Case Study for the Trimethylaluminum/Water Process. *J. Appl. Phys.* **2005**, *97*, 9. [CrossRef]
10. An, J.; Choi, K.K.; Kang, B.; Baek, R.H. Curing Defects in Plasma-Enhanced Atomic Layer Deposition of Al_2O_3 by Six Methods. *Mater. Sci. Semicond. Process.* **2022**, *152*, 107070. [CrossRef]
11. Sacchettini, Y.; Carrère, J.P.; Doyen, C.; Duru, R.; Courouble, K.; Ricq, S.; Goiffon, V.; Magnan, P. A Highly Reliable Back Side Illuminated Pixel against Plasma Induced Damage. *Int. Electron Devices Meet. IEDM* **2019**, *382*, 16.5.1–16.5.4. [CrossRef]
12. Hoex, B.; Gielis, J.J.H.; Van de Sanden, M.C.M.; Kessels, W.M.M. On the c-Si surface passivation mechanism by the negative-charge-dielectric Al_2O_3. *J. Appl. Phys.* **2008**, *104*, 113703. [CrossRef]
13. Liu, D.; Robertson, J. Oxygen Vacancy Levels and Interfaces of Al_2O_3. *Microelectron. Eng.* **2009**, *86*, 1668–1671. [CrossRef]
14. Uren, M.H.; Stathis, J.H.; Cartier, E. Conductance Measurements on Pb Centers at the (111) Si:SiO_2 Interface. *J. Appl. Phys.* **1996**, *80*, 3915. [CrossRef]
15. Schmidt, J.; Veith, B.; Werner, F.; Zielke, D.; Brendel, R. Silicon Surface Passivation by Ultrathin Al_2O_3 Films and Al_2O_3/SiN_x Stacks. In Proceedings of the 35th IEEE Photovoltaic Specialists Conference, Honolulu, HI, USA, 20–25 June 2010; pp. 885–890. [CrossRef]
16. Naumann, V.; Otto, M.; Wehrspohn, R.B.; Werner, M.; Hagendorf, C. Interface and Material Characterization of Thin ALD-Al_2O_3 Layers on Crystalline Silicon. *Energy Procedia* **2012**, *27*, 312–318. [CrossRef]
17. Gakis, G.P.; Vahlas, C.; Vergnes, H.; Dourdain, S.; Tison, Y.; Martinez, H.; Bour, J.; Ruch, D.; Boudouvis, A.G.; Caussat, B.; et al. Investigation of the Initial Deposition Steps and the Interfacial Layer of Atomic Layer Deposited (ALD) Al_2O_3 on Si. *Appl. Surf. Sci.* **2019**, *492*, 245–254. [CrossRef]
18. Jakschik, S.; Schroeder, U.; Hecht, T.; Gutsche, M.; Seidl, H.; Bartha, J.W. Crystallization Behavior of Thin ALD-Al_2O_3 Films. *Thin Solid Films* **2003**, *425*, 216–220. [CrossRef]
19. Piskorski, K.; Przewlocki, H.M. The Methods to Determine Flat-Band Voltage V_{FB} in Semiconductor of a MOS Structure. In Proceedings of the 33rd International Convention MIPRO, Opatija, Croatia, 24–28 May 2010; pp. 37–42.

20. Birey, H. Thickness Dependence of the Dielectric Constant and Resistance of Al_2O_3 Films. *J. Appl. Phys.* **1977**, *48*, 5209–5212. [CrossRef]
21. Choi, M.; Lyons, J.L.; Janotti, A.; Van De Walle, C.G. Impact of Carbon and Nitrogen Impurities in High-κ Dielectrics on Metal-Oxide-Semiconductor Devices. *Appl. Phys. Lett.* **2013**, *102*, 142902. [CrossRef]
22. Langereis, E.; Keijmel, J.; Van de Sanden, M.C.M.; Kessels, W.M.M. Surface chemistry of plasma-assisted atomic layer deposition of studied by infrared spectroscopy. *Appl. Phys. Lett.* **2008**, *92*, 231904. [CrossRef]
23. Mahajan, A.M.; Khairnar, A.G.; Thibeault, B.J. Electrical Properties of MOS Capacitors Formed by PEALD Grown Al_2O_3 on Silicon. *Semiconductors* **2014**, *48*, 497–500. [CrossRef]
24. Kim, J.; Bang, S.; Lee, S.; Shin, S.; Park, J.; Seo, H.; Jeon, H. A Study on H_2 Plasma Treatment Effect on A-IGZO Thin Film Transistor. *J. Mater. Res.* **2012**, *27*, 2318–2325. [CrossRef]
25. Lebreton, F.; Abolmasov, S.N.; Silva, F.; Roca, P. In situ photoluminescence study of plasma-induced damage at the a-Si:H/c-Si interface. *Appl. Phys. Lett.* **2016**, *108*, 051603. [CrossRef]